View Article Online
DOI: 10.1039/C7AN00436B

Impedimetric measurement of DNA-DNA hybridisation using microelectrodes with different radii for detection of methicillin resistant *Staphylococcus aureus* (MRSA).

Poh Quan Li[1&2], Andrew Piper[2], Ilka Schmueser[3] Andrew, R Mount[2] and Damion K Corrigan[4]

[1] Nanyang Technological University, Singapore.

[2] EASTCHEM, School of Chemistry, The University of Edinburgh, Joseph Black Building, The King's Buildings, West Mains Road, Edinburgh, EH9 3JJ, Scotland (UK)

[3] Institute for Integrated Micro and Nano Systems, School of Engineering, The University of Edinburgh, The King's Buildings, West Mains Road, Edinburgh EH9 3JF, Scotland (UK)

[4] Department of Biomedical Engineering, University of Strathclyde, Glasgow, G4 0NS.

Corresponding author – Dr Damion Corrigan – damion.corrigan@strath.ac.uk

Abstract

Due to their electroanalytical advantages, microelectrodes are a very attractive technology for sensing and monitoring applications. One highly important application is measurement of DNA hybridisation to detect a wide range of clinically important phenomena, including single nucleotide polymorphisms (SNPs), mutations and drug resistance genes. The use of electrochemical impedance spectroscopy (EIS) for measurement of DNA hybridisation is well established for large electrodes but as yet remains relatively unexplored for microelectrodes due to difficulties associated with electrode functionalisation and impedimetric response interpretation. To shed light on this, microelectrodes were initially fabricated using photolithography and characterised electrochemically to ensure their responses matched established theory. Electrodes with different radii (50, 25, 15 and 5 μm) were then functionalised with a mixed film of 6-mercapto-1-hexanol and a thiolated single stranded ssDNA capture probe for a specific gene from the antibiotic resistant bacterium MRSA. The complementary oligonucleotide target from the *mecA* MRSA gene was hybridised with the surface tethered ssDNA probe. The EIS response was evaluated as a function of electrode radius and it was found that charge-transfer (R_{CT}) was more significantly affected by hybridisation of the *mecA* gene than the non-linear resistance (R_{NL}) which is associated with the steady state current. The discrimination of *mecA* hybridisation improved as electrode radius reduced with the R_{CT} component of the response becoming increasingly dominant for smaller radii. It was possible to utilise these findings to produce a real time measurement of oligonucleotide binding where changes in R_{CT} were evident one minute after nanomolar target addition. These data provide a systematic account of the effect of microelectrode radius on the measurement of hybridisation, providing insight into critical aspects of sensor design and implementation for the measurement of clinically important DNA sequences. The findings open up the possibility of developing rapid, sensitive DNA based measurements using microelectrodes.

Introduction

Chemical and biochemical sensing is vital for diagnosis of medical conditions[1], detection of pathogens[2], monitoring of water quality[3] and industrial processes[4]. Detection of specific

View Article Online
DOI: 10.1039/C7AN00436B

genetic sequences enables rapid profiling of clinical samples for evidence of disease, e.g. antibody/antigenic biomarkers or presence of antibiotic resistant bacteria. Electrochemical impedance spectroscopy (EIS) is a powerful measurement technique which provides information on a number of physical processes taking place at an electrified interface. Processes which can be probed using EIS include: double layer capacitance, electron transfer, diffusional phenomena etc. and because the technique does not require the target molecule to be labelled it has potential for use at the point of care.

Microelectrodes have the electroanalytical advantages of reduced *iR* drop, improved signal to noise ratio, insensitivity to convection and the ability to be produced in individually addressable arrays. They offer a number of advantages over macroelectrodes for electrochemical sensing[5] in chemical[3], industrial[6,7] and medical applications[8]. These advantages make microelectrodes and arrays of microelectrodes an attractive technology for sensitive and specific detection of biomarkers. To harness these advantages, particularly for EIS measurements, it is necessary to fully characterise microelectrode based measurements of DNA hybridisation. Photolithographic techniques from the silicon semiconductor industry are particularly attractive for microelectrode fabrication due to the ability to produce with high precision and reproducibility metallic structures and insulating layers with well-defined shapes and dimensions[9]. Here, these techniques were employed for fabrication of well-defined disc microelectrodes with high reproducibility.

Electrochemical impedance spectroscopy (EIS) involves the use of an AC voltage peturbation at the working electrode and measurement of the resulting current. The technique can be performed in a Faradaic manner (with the use of a redox couple) and in a non-Faradaic manner and parameters such as the solution resistance (R_S), double layer capacitance (C_{DL}), charge transfer resistance (R_{CT}) and Warburg impedance (W) can be extracted from the response. In nucleic acid detection, a common approach is to use the negatively charged redox couple potassium ferri-ferrocyanide for the measurement of R_{CT} upon DNA recognition[10]. EIS has been used to detect DNA-DNA recognition at an electrode surface and numerous biosensors have been developed using this measurement approach in concert with a wide range of electrode types[11–14]. Specifically, for the detection of nucleic acids, studies have demonstrated the successful fabrication of microelectode devices using photolithographic methods and the development of nucleic acid sensors which use EIS as the measurement technique. Examples include the detection of BRCA1 gene in breast cancer using interdigitated electrodes[15] the measurement of matched an mismatched DNA for detection of mutations[16] the measurement of 16SrRNA for antibiotic susceptibility testing[17] and the detection of West Nile virus using interdigitated microelectrodes[18].

Antimicrobial resistance is a major scientific challenge of the day. The United Nations and the World Health Organisation have publicised the need for urgent, coordinated, global action in the fight against emerging rates of resistance. Recently, there have been reports in the literature of emergence of resistance to the antibiotic of last resort in the United States[19]. In the effort to counter antimicrobial resistance (AMR) it is important to both develop new antibiotics and achieve improved stewardship over existing drugs. A key aspect of improving antibiotic stewardship is developing rapid diagnostic tests and electrochemical sensors represent a potentially useful technology for rapidly detecting resistance and informing clinicians of which antibiotics to prescribe and whether isolation of the patient is necessary. Resistance to methicillin and in particular the emergence of the methicillin resistant *Staphylococcus aureus* (MRSA) strain has been a major problem in both healthcare acquired and community acquired drug resistant infections[20]. Methicillin resistance relies primarily on the organism having acquired the *mecA* gene which codes for penicillin binding protein 2A

View Article Online
DOI: 10.1039/C7AN00436B

(PBP2A)[21]. Detection of the mecA gene sequence confirms methicillin resistance and in this study, a probe sequence for the *mecA* gene was employed for electrochemical detection of short oligonucleotides. The paper demonstrates the advantageous nature of using microelectrodes with smaller radii for the detection of such DNA sequences and brings to light the possibility of utilising microelectrode sensors for routine clinical detection purposes.

Materials and Methods

Microfabrication of electrode devices

The microelectrode devices were produced using reliable, well-characterised silicon based microfabrication processes (Figure 1). Initially, a 500 nm thick layer of silicon dioxide insulation was grown on silicon wafer substrates. Next, a 20 nm thick film of titanium nitride was deposited onto the surface as an adhesion layer for the electrode metal which was a 50 nm film of platinum. Patterning of the electrode metal layer was then achieved by reactive ion etching, using photolithographic masking to prevent the exposure of a band of metal around the perimeter of each device when diced. Subsequent deposition of a 500 nm thick layer of silicon nitride produced a top insulator, which was again patterned using photolithographic masking and reactive ion etching of the insulator to expose the bond pad and the microelectrode. Detailed accounts of the electrode fabrication process can be found in a previous publication[22].

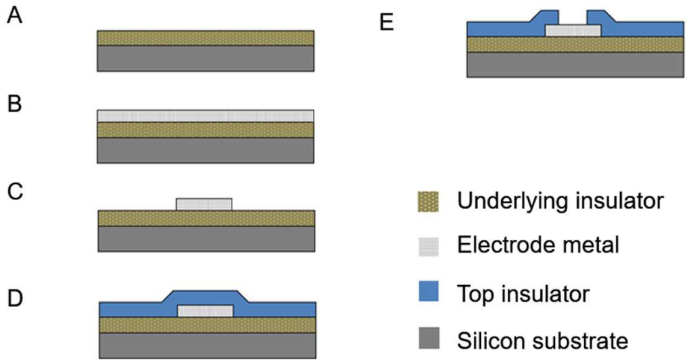

Figure 1. Depiction of the microfabrication processes used for electrode production.

Electrode preparation and DNA sequences

The DNA sequences employed in this study are shown in table 1 and were developed as part of a previous study along with a detailed protocol for the immobilisation of the mixed thiol probe film[23]. To summarise, the mixed layer of 6-mercapto-1-hexanol (30 µM) and a thiolated ssDNA probe (1.5 µM) was prepared on the sensor surface by overnight incubation with a mixed solution followed by a 1 hour "blocking" step in 1.0 mM 6-mercapto-1-hexanol solution to remove unbound ssDNA molecules and to ensure upright orientation of the capture probe. Tris(2-carboxyethyl) phosphine was added to both the probe immobilisation solution and back filling solution at 50 mM concentration to promote cleavage of dithiol bonds[24]. Probe modified microelectrodes were electrochemically characterised using the

View Article Online
DOI: 10.1039/C7AN00436B

ferri-ferrocyanide redox couple and then incubated with 100 nM solutions of DNA before electrochemical measurements were repeated.

Table 1 – DNA sequences employed in this study

	Oligo name	3' Modif.	5' Modif.	Sequence 5'-3'
1	30 mer *mecA* target	-	-	GTATGCTTTGGTCTTTCTGCATTCCTGGAA
2	Non complementary	-	-	GTACTGAGTAATACC
2	PNA MRSA *mecA* capture probe	-	3.8 nm - Thiol-C11-AEEEA	TTCCAGGAATGCAGA

Electrochemical measurements

Cyclic voltammetry (CV) and Electrochemical Impedance Spectroscopy (EIS) measurements were performed in a measurement buffer consisting of various concentrations of potassium ferrocyanide, potassium ferricyanide, and potassium chloride as the supporting electrolyte. CV measurements were performed using a platinum counter electrode and a saturated $Ag/AgCl/Cl^-$ reference electrode. EIS measurements were performed by superimposing an AC potential of 10 mV rms onto the open circuit potential over a frequency range of 100 kHz to 0.1 Hz and measuring the current response. Thirty frequencies were measured and frequency values were selected on a logarithmic basis. Nyquist plots were produced (Z' vs –Z'') and circuit fitting was performed in order to extract values for the different circuit elements of an equivalent circuit.

Results & Discussion

Electrochemical characterisation of unmodified microelectrodes

Initially, electrochemical responses from Pt microelectrodes with different radii were recorded using cyclic voltammetry. CV experiments were performed in a solution of 5.0 mM potassium ferrocyanide + 10 mM potassium chloride. Figure 2A shows the voltammetric response with the limiting currents for the oxidation of potassium ferrocyanide to ferricyanide how they were reduced as electrode radius decreased. The responses observed in these voltammograms were typical of microelectrodes, in that a "steady state" CV was recorded with sweep rate independence observed.

Equation 1 has been shown to describe the limiting current for a microdisc electrode[5]:

$$i_L = 4nFDcr \qquad (1)$$

where i_L is the limiting current, n is the number of electrons transferred, F is Faraday's constant, D is the diffusion coefficient, c is the concentration of the redox species and r is the electrode radius. From equation 1, an example value of $D = 6.85\times10^{-6}$ cm^2s^{-1} (298 K) was calculated for potassium ferrocyanide using the r = 25 µm disc, which corresponded favourably to literature values (e.g. 6.3×10^{-6} cm^2 s^{-1} at 298 K^{25} - it is important to note a wide variation in the literature for diffusion coefficients of the ferri-ferrocyanide couple). As can be seen in figure 2A the limiting current scaled with electrode radius as predicted by equation

View Article Online
DOI: 10.1039/C7AN00436B

1. It is reassuring and satisfying that these photolithographically fabricated microelectrodes showed the expected response prior to chemical modification and *mecA* detection experiments. Reductions in current observed immediately upon reversing the bias can be attributed to parasitic capacitances from microfabricated structures[26]. Figure 2B presents a microscope image of an r = 25 µm electrode (diameter = 50 µm) and shows a platinum disc defined by the silicon nitride insulating layer.

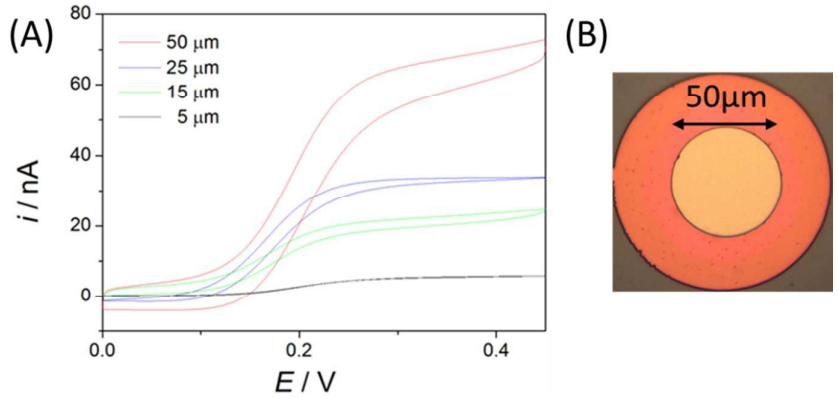

Figure 2. (A) CVs recorded at electrodes with radii 5. 15, 20 and 50 µm in 5 mM potassium ferrocyanide + 10 mM potassium chloride prior to immobilisation of the sensing film. (B) Microscope image of a r = 25 µm Pt disc microelectrode produced using photolithographic microfabrication techniques.

Impedimetric response following formation of a self-assembled monolayer (SAM) and microelectrode based detection of the *mecA* antimicrobial resistance gene.

Next, investigations were performed where a sensing probe film was immobilised onto the electrode surface by incubation in a solution containing a thiolated DNA probe sequence for the *mecA* gene and 6-mercapto-1-hexanol. In these experiments the probe-film immobilised electrodes were subjected to an initial EIS measurement in order to record the pre-hybridsation response. The electrodes were then incubated in 100 nM *mecA* target DNA + 10 mM KCl solution for 20 minutes to allow DNA hybridisation, followed by a stringency wash in 1 mM KCl to remove any non-specifically bound DNA before a final EIS measurement to characterise the electrode post hybridisation. The results of these measurements can be seen in Figure 3A-D where EIS responses of clean, pre-hybridisation and post-hybridisation microelectrodes with four different radii (50, 25, 15 and 5 µm) are shown. The most obvious trend is the increase in the "impedance" as each electrode is sequentially modified, i.e. R_{CT} increased as the electrode was first modified with capture probe and then following hybridisation of target DNA. This initial observation was not entirely expected since there are a number of varying reports in the literature on the impedimentric behaviour of micro and nano electrode DNA sensors. In the presence of ferri/ferrocyanide as a redox mediator there are accounts of both increased [16] and decreased R_{CT} values [27] upon target DNA binding. These reports attribute the observed change in the impedimetric response to the sensing film structure and the resulting conformational/structural changes which occur on the surfaces of electrodes with different geometries[27]. In this study, the protocol used to prepare the sensor surface resulted in a film conformation which caused an increase in R_{CT} following target binding, which was in keeping with previous macroelectrode studies where increases in R_{CT}

View Article Online
DOI: 10.1039/C7AN00436B

were attributed to the target DNA blocking pinholes and increasing electrostatic repulsion at the electrode surface, ultimately causing a decrease in the exchange current density[28].

The second most obvious thing to note from figure 3 is the changing nature and magnitude of the impedimetric response as electrode radius decreased, i.e. the merging of the R_{CT} and R_{NL} semi-circles and the overall increase in resistance as *r* decreased. For *r* = 50 µm electrodes (figure 3D) there were two distinct semi-circles with the first originating from R_{CT} and the second from R_{NL} (which is characteristic of the limiting current (i_L) established following the evolution of a hemispherical diffusion profile). As electrode radius decreased, the first semi-circle, i.e. that associated with R_{CT}, increased, as would be expected since R_{CT} is inversely proportional to electrode area. This can be seen from the circuit fit values shown in table 2 (equivalent circuits shown in figures 4B & C), where, the increased magnitude of the R_{CT} semi-circle made it difficult to obtain a realistic fit for R_{NL} because the steady state current was responsible for a smaller proportion of the overall response. As the electrode radius decreased the relative contribution of R_{CT} increased and in the case of the *r* = 5 µm electrode the response was almost entirely one single semi-circle (see figure 3A). As shown in Figure 3A and Table 2, the equivalent circuit had to be amended as both the electrode radius decreased and as the electrode was modified with first probe and second target DNA. It was necessary to fit the *r* = 5 µm response with a Randles' circuit – see figure 4C. It was also necessary to fit the probe + DNA target response for *r* = 15 µm with the same orthodox Randle's circuit. It is noteworthy that as the radius of the microfabricated sensor reduced and as the electrode was increasingly modified the *'goodness of fit'* for the modified Randles' circuit (see figure 4B) decreased, again demonstrating the importance of the R_{CT} reaction and its relative dominance over R_{NL} in the microelectrode response[29]. Finally, from figure 3A-D and table 2 it can be seen that R_{NL} was not a reliable parameter for assessing DNA hybridisation and the changing nature of the surface, the pattern of consistent increases seen for R_{CT} was not observed with R_{NL} and for electrodes with smaller radii it was difficult to obtain an accurate value from circuit fitting due to the relative dominance of R_{CT}.

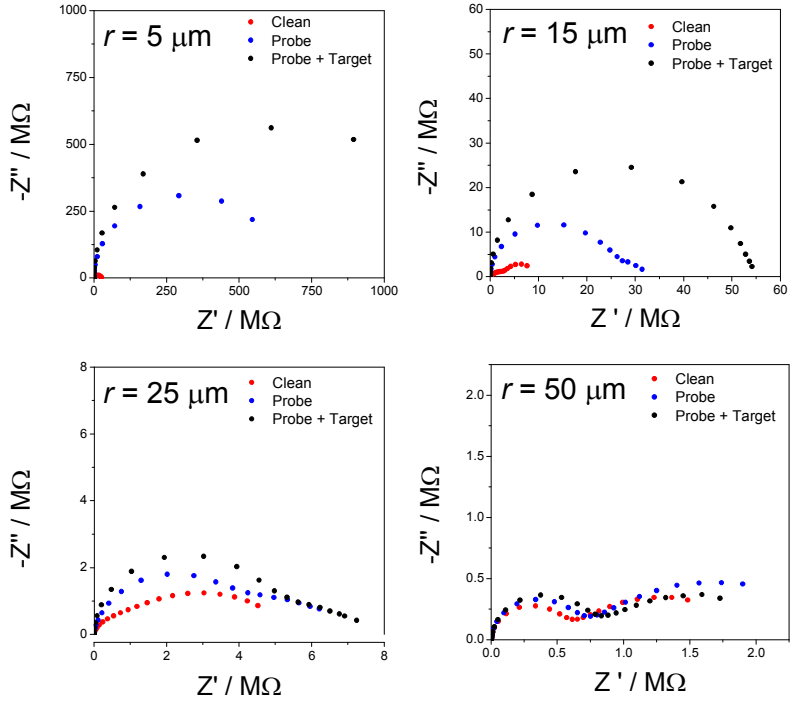

View Article Online
DOI: 10.1039/C7AN00436B

Figure 3. EIS response from microelectrodes of four different radii (A) 5 µm (B) 10 µm (C) 25 µm and (D) 50 µm after cleaning, probe functionalisation and target binding recorded at open circuit in a measurement buffer containing 1 mM potassium ferri-ferrocyanide + 10 mM KCl.

Table 2. Fitted values and errors for R_{CT} and R_{NL} and global χ^2 for EIS fits recorded at microelectrodes with r = 50, 25, 15 and 5 µm

	R_{CT} (MΩ)	Error (%)	R_{NL}(MΩ)	Error (%)	χ^2
***r* = 50**	0.12	2.75	1.96	1.54	1.51×10^{-2}
Probe	0.51	0.96	1.68	1.23	8.30×10^{-3}
Target	0.69	1.00	1.77	1.60	1.09×10^{-2}
***r* = 25**	0.36	7.89	5.52	0.52	4.34×10^{-3}
Probe	2.94	2.46	4.28	1.584	1.04×10^{-2}
Target	4.35	1.90	3.39	2.34	1.52×10^{-2}
***r* = 15**	1.09	12.8	13.54	5.76	2.30×10^{-1}
Probe	21.4	4.16	11.73	5.99	3.62×10^{-2}
Target	52.5	0.71	-	-	5.44×10^{-2}
***r* = 5**	24.5	1.79	-	-	3.33×10^{-1}
Probe	627	0.47	-	-	8.93×10^{-3}
Target	1160	0.71	-	-	9.70×10^{-3}

Figure 4 shows a plot of R_{CT} × Area vs electrode radius and is in effect a normalisation to account for electrode area. The plot importantly indicates that as radius decreased the magnitude of the signal change between clean, probe immobilised and DNA target bound electrodes increased demonstrating that microelectrodes with smaller radii showed enhanced performance at discriminating first the immobilisation of the probe film and second the binding of the *mecA* DNA target sequence. Crucial to the explanation of this was the observation that a decrease in electrode radius from 50 to 5 µm caused the limiting current to reduce by a factor of ten (as shown in figure 2 and predicted by equation 1). Equation 2 describes how the limiting current is related to the non-linear resistance (R_{NL}) and therefore is governed primarily by the electrode radius. As a result, the limiting current was influenced less by capture probe immobilisation and target DNA addition than the R_{CT} reaction (see figure S1 in supplementary information which shows CV responses for DNA modified microelectodes). When the radius decreased from 50 to 5 µm, the electrode area changed by a factor of one hundred and since the surface based redox reaction is influenced by the area of the electrode (see equation 3)[30], a larger, more apparent change in R_{CT} was observed than for R_{NL}. The results presented in figure 4 and the fitted values displayed in Table 2 show that as the electrode radius decreased the surface based R_{CT} reaction dominated the response and for smaller radii showed enhanced discrimination of DNA target binding.

$$R_{NL} = \frac{4RT}{nFi_L} \text{ (equation 2)}$$

Where R is universal gas constant, T is temperature, F is Faraday's constant and i_L is limiting current.

$$R_{CT} = \frac{4RTL}{nAF^2c_\infty} \text{ (equation 3)}$$

View Article Online
DOI: 10.1039/C7AN00436B

Where R is universal gas constant, T is temperature, L is the diffusion length, F is Faraday's constant c_∞ is bulk concentration and A is the electrode area.

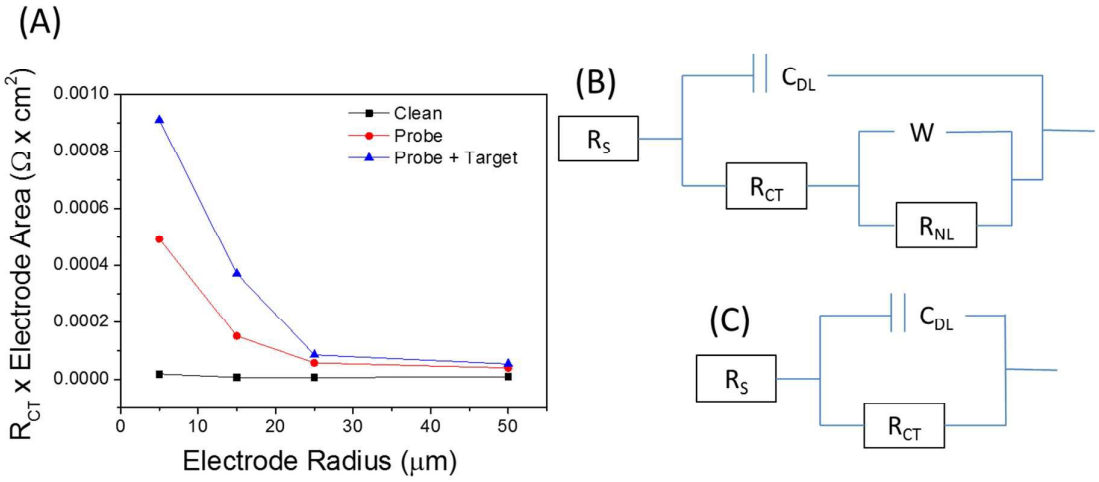

Figure 4. (A) Plot of R_{CT} × electrode area vs electrode radius for electrodes following cleaning, probe functionalisation and target binding. (B) Modified Randles' circuit for microelectrodes. (C) Randles' equivalent circuit.

Our previous studies involving nucleic acid macroelectrode sensors have not shown improvements in sensitivity through reduction of electrode area and for microelectrode based DNA sensors there are no systematic reports in the literature on the effect of radius on the impedimetric measurement. The data presented here demonstrate a clear trend of increasing dominance of R_{CT} in the impedimetric response at microelectrodes as radius is reduced and that for greatest discrimination of DNA hybridisation, a radius of 5-15 μm was optimal which, is well within the resolution limits of standard photolithographic approaches and for use in multi-electrode arrays. Having developed a number of macroelectrode based bioassays for AMR [31–34] and infection biomarkers[35] with limits of detection in the pM to fM range and with high specificity for AMR genes such as the *mecA* sequence[29&30], it will now be possible to utilise the well-known electroanalytical advantages of microelectrodes to improve performance of this clinically relevant assay.

Finally, and having shown that reducing the electrode radius improved the resolution of DNA-DNA hybridisation an r = 15 μm electrode was used to perform measurement of ssDNA *mecA* target binding with the surface tethered capture probe in real time. In this experiment the microelectrode was used to record EIS measurements in a continuous fashion. The frequency range was selected using the impedimetric response obtained and initially displayed in figure 3C and the protocol designed to record an impedance measurement every minute. After 6 minutes of measurements, complementary and non-complementary DNA target strands were added at a concentration of 10 nM (arrows) which is above the limits of detection for the DNA sequence established in previous reports[30]. Following addition of the ssDNA oligonucleotide target a change in R_{CT} was apparent after one minute with hybridisation of the target following the expected binding isotherm. This result demonstrates an approach to rapidly measuring binding of an oligonucleotide sequence from an antibiotic resistance gene in real time using a microelectrode and paves the way for the use of microelectrode arrays for the measurement of several resistance genes on a single multi-microelectrode chip. It is also important to note that in previous studies which developed this *mecA* detection system, macroelectrodes were employed and consideration was given to

View Article Online
DOI: 10.1039/C7AN00436B

sample preparation, probe design & sequence and aspects of sample handling & processing which allowed for the rapid detection of MRSA in human wound fluid in less than 30 minutes[33]. Specificity was given consideration and of particular importance was the DNA probe sequence, which was selected using a microarray to screen potential sequences[34] for optimum binding of the *mecA* sequence. Figures 6B & S2 show the effect of adding non-complementary DNA to a functionalised microelectrode and it can be observed that a negligible increase in R_{CT} was seen after one hour showing that the specificity of the assay had been preserved when transferred from macro to microelectrode. The detection sensitivity reported here is at least equivalent and with development of the microelectrode measurement and measuring longer DNA strands from clinical samples it will lead to sensitivity gains using the new protocol.

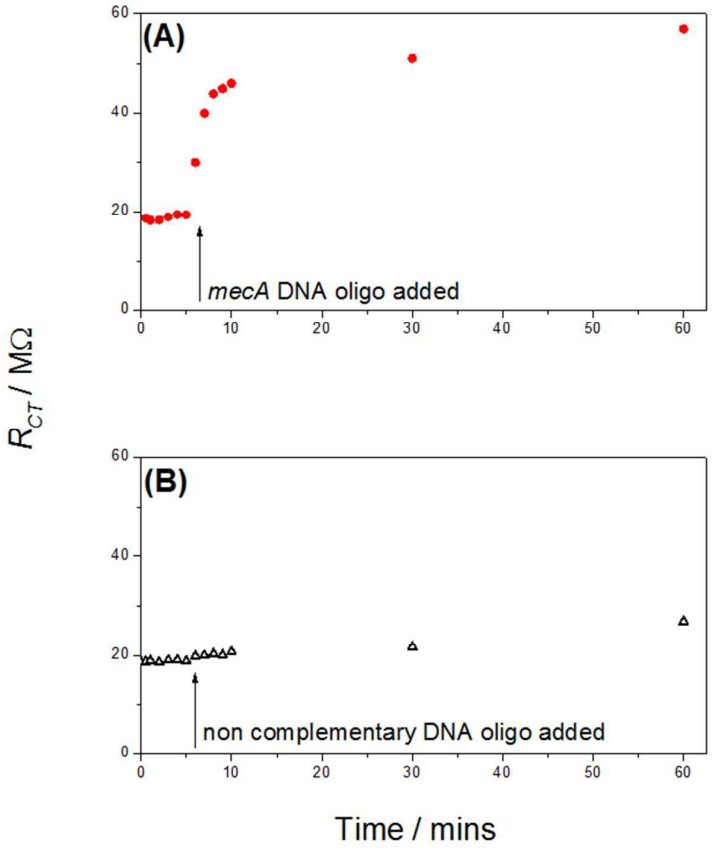

Figure 6. Binding of the *mecA* MRSA oligonucleotide (A) and a non-complementary sequence (B) measured in real time by continuous EIS. Recorded using a microelectrode (r = 15 µm) at open circuit in a measurement solution of 0.1 mM potassium ferri-ferrocyanide + 10 mM KCl. Both oligonucleotides were added at a concentration of 10 nM.

Conclusions

Using photolithographic microfabrication techniques, it was possible to produce microelectrode discs with well-defined radii which gave the expected limiting currents and diffusion coefficients for potassium ferrocyanide. These electrodes were functionalised with a ssDNA capture probe and used to bind a complementary ssDNA oligonucleotide target

View Article Online
DOI: 10.1039/C7AN00436B

from the *mecA* gene. The microelectrode response initially consisted of two semi circles, the first characteristic of the surface based R_{CT} reaction and the second characteristic of the steady state current denoted R_{NL}. Equivalent circuit fitting showed that R_{CT} changed predictably and consistently with binding of the *mecA* gene and the greatest signal increases came from electrodes with smaller radii. R_{NL} was found to show little change following electrode modification with ssDNA capture probe and following target DNA binding. As electrode radius decreased it was difficult to obtain realistic fits for R_{NL} with R_{CT} increasingly dominating the response. In these cases it was necessary to fit with the well-established Randles' circuit. Following optimisation of the measurement and selection of suitable conditions it was then possible to use the microelectrode to rapidly detect the binding of single stranded *mecA* oligonucleotide DNA in less than one minute, demonstrating the possible use of the microelectrode sensor for the detection of methicillin resistance in clinical isolates. These data highlight some of the important issues in developing microelectrodes for detection of nucleic acid hybridisation from clinical samples. Having shown the critical importance of electrode radius and response interpretation for actualising a microelectrode measurement, it is now our intention to develop individually addressable arrays for a number of clinically important measurements, including pathogen identification, resistance gene detection and measurement of clinically important DNA mutations.

Acknowledgements

DC would like to thank the Advanced Forming Research Centre (AFRC), University of Strathclyde for Route to Impact Funding and the Dowager Countess Eleanor Peel Trust for a Minor Medical Grant. In addition, DC would like to thank Dylan Bennett for performing preliminary experiments and Ewen Blair for useful discussions on microfabrication.

References

1 S. Liébana, L. J. Jones, G. A. Drago, R. W. Pittson, D. Liu, W. Perrie and J. P. Hart, *Sensors Actuators B Chem.*, 2016, **231**, 384–392.

2 M. K. Patel, P. R. Solanki, S. Seth, S. Gupta, S. Khare, A. Kumar and B. D. Malhotra, *Electrochem. commun.*, 2009, **11**, 969–973.

3 M. Sosna, G. Denuault, R. W. Pascal, R. D. Prien and M. Mowlem, *Sensors Actuators, B Chem.*, 2007, **123**, 344–351.

4 D. K. Corrigan, N. A. Salton, C. Preston and S. Piletsky, *J. Pharm. Pharmacol.*, 2010, **62**, 1195–1200.

5 B. J. Heinze, *Agnew Chem Int Ed*., 1993, **32**, 1268-1288.

6 D. K. Corrigan, E. O. Blair, J. G. Terry, A. J. Walton and A. R. Mount, *Anal. Chem.*, 2014, **86**, 11342–11348.

7 D.K. Corrigan, J.P. Elliott, E.O. Blair, S.J. Reevea, I Schmueser, A.J.W. Walton and A.R.Mount. *Faraday Discuss.*, 2016, 351–366.

8 J. Zhou, L. Zhang and Y. Tian, *Anal. Chem.*, 2016, **88**, 2113–2118.

View Article Online
DOI: 10.1039/C7AN00436B

9 R. G. Compton, X. Huang, A. M. O. Mahony and R. G. Compton, 2009, 776–788.

10 F. Lisdat and D. Schäfer, *Anal. Bioanal. Chem.*, 2008, **391**, 1555–1567.

11 M. Riedel, J. Kartchemnik, M. J. Schöning and F. Lisdat, *Anal. Chem.*, 2014, **86**, 7867–7874.

12 J. Kafka, O. Pänke, B. Abendroth and F. Lisdat, *Electrochim. Acta*, 2008, **53**, 7467–7474.

13 N. Tercero, K. Wang, P. Gong and R. Levicky, *JACS*, 2009, **131**, 4953-4961..

14 N. Zhu, H. Gao, Q. Xu, Y. Lin, L. Su and L. Mao, *Biosens. Bioelectron.*, 2010, **25**, 1498–1503.

15 A. Bonanni, I. Fernández-Cuesta, X. Borrisé, F. Pérez-Murano, S. Alegret and M. del Valle, *Microchim. Acta*, 2010, **170**, 275–281.

16 X. Li, J. S. Lee and H. B. Kraatz, *Anal. Chem.*, 2006, **78**, 6096–6101.

17 T. Liu, Y. Lu, V. Gau, J. C. Liao and P. K. Wong, *Ann. Biomed. Eng.*, 2014, **42**, 2314–2321.

18 L. Wang, M. Veselinovic, L. Yang, B. J. Geiss, D. S. Dandy and T. Chen, *Biosens. Bioelectron.*, 2017, **87**, 646–653.

19 P. McGann, E. Snesrud, R. Maybank, B. Corey, A. C. Ong, R. Clifford, M. Hinkle, T. Whitman, E. Lesho and K. E. Schaecher, *Antimicrob. Agents Chemother.*, 2016, **60**, AAC.01103-16.

20 P. D. Stapleton and P. W. Taylor, 2007, *Sci Prog* **85**, 1–14.

21 S. J. Peacock and G. K. Paterson, *Annu. Rev. Biochem.*, 2015, **84**, 577–601.

22 E. O. Blair, D. K. Corrigan, J. G. Terry, A. R. Mount and A. J. Walton, *J. Microelectromechanical Syst.*, 2015, **24**, 1346–1354.

23 D. K. Corrigan, H. Schulze, R. A. McDermott, I. Schm??ser, G. Henihan, J. B. Henry, T. T. Bachmann and A. R. Mount, *J. Electroanal. Chem.*, 2014, **732**, 25–29.

24 D. K. Corrigan, H. Schulze, I. Ciani, G. Henihan, A. R. Mount and T. T. Bachmann, *J. Electroanal. Chem.*, 2017, **786**, 58–62.

25 R. O. Kadara, N. Jenkinson and C. E. Banks, *Sensors Actuators, B Chem.*, 2009, **138**, 556–562.

26 I. Schmueser, A. J. Walton, J. G. Terry, H. L. Woodvine, N. J. Freeman and A. R. Mount, *Faraday Discuss.*, 2013, **164**, 295.

27 G. Liu, C. Sun, D. Li, S. Song, B. Mao, C. Fan and Z. Tian, *Adv. Mater.*, 2010, **22**, 2148–2150.

28 S. D. Keighley, P. Estrela, P. Li and P. Migliorato, *Biosens. Bioelectron.*, 2008, **24**, 906–911.

29 D. Li, X. Zou, Q. Shen and S. Dong, *Electrochem. commun.*, 2007, **9**, 191–196.

View Article Online
DOI: 10.1039/C7AN00436B

30 H. L. Woodvine, J. G. Terry, A. J. Walton and A. R. Mount, *Analyst*, 2010, **135**, 1058–1065.

31 J. M.-Y. Huang, G. Henihan, D. Macdonald, A. Michalowski, K. Templeton, A. P. Gibb, H. Schulze and T. T. Bachmann, *Anal. Chem.*, 2015, **87** 7738-45.

32 G. Henihan, H. Schulze, D. K. Corrigan, G. Giraud, J. G. Terry, A. Hardie, C. J. Campbell, A. J. Walton, J. Crain, R. Pethig, K. E. Templeton, A. R. Mount and T. T. Bachmann, *Biosens. Bioelectron.*, 2016, **81**, 487–494.

33 D. K. Corrigan, H. Schulze, G. Henihan, a Hardie, I. Ciani, G. Giraud, J. G. Terry, A. J. Walton, R. Pethig, P. Ghazal, J. Crain, C. J. Campbell, K. E. Templeton, A R. Mount and T. T. Bachmann, *Analyst*, 2013, **138**, 6997–7005.

34 D. K. Corrigan, H. Schulze, G. Henihan, I. Ciani, G. Giraud, J. G. Terry, A. J. Walton, R. Pethig, P. Ghazal, J. Crain, C. J. Campbell, A. R. Mount and T. T. Bachmann, *Biosens. Bioelectron.*, 2012, **34**, 178–184.

35 I. Ciani, H. Schulze, D. K. Corrigan, G. Henihan, G. Giraud, J. G. Terry, A. J. Walton, R. Pethig, P. Ghazal, J. Crain, C. J. Campbell, T. T. Bachmann and A. R. Mount, *Biosens. Bioelectron.*, 2012, **31**, 413–418.

View Article Online
DOI: 10.1039/C7AN00436B

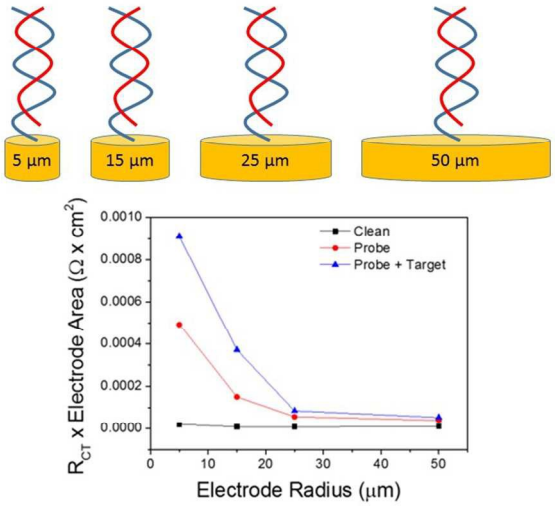

338x190mm (96 x 96 DPI)

Supplementary Information

Impedimetric measurement of DNA-DNA hybridisation using microelectrodes with different radii for detection of methicillin resistant *Staphylococcus aureus* (MRSA).

Poh Quan Li[1] and Damion K Corrigan[2]

[1] EastCHEM, School of Chemistry, The University of Edinburgh, Joseph Black Building, The King's Buildings, West Mains Road, Edinburgh, EH9 3FJ, Scotland (UK)

[2] Department of Biomedical Engineering, University of Strathclyde, Glasgow, G4 0NS.

Corresponding author – Dr Damion Corrigan – damion.corrigan@strath.ac.uk

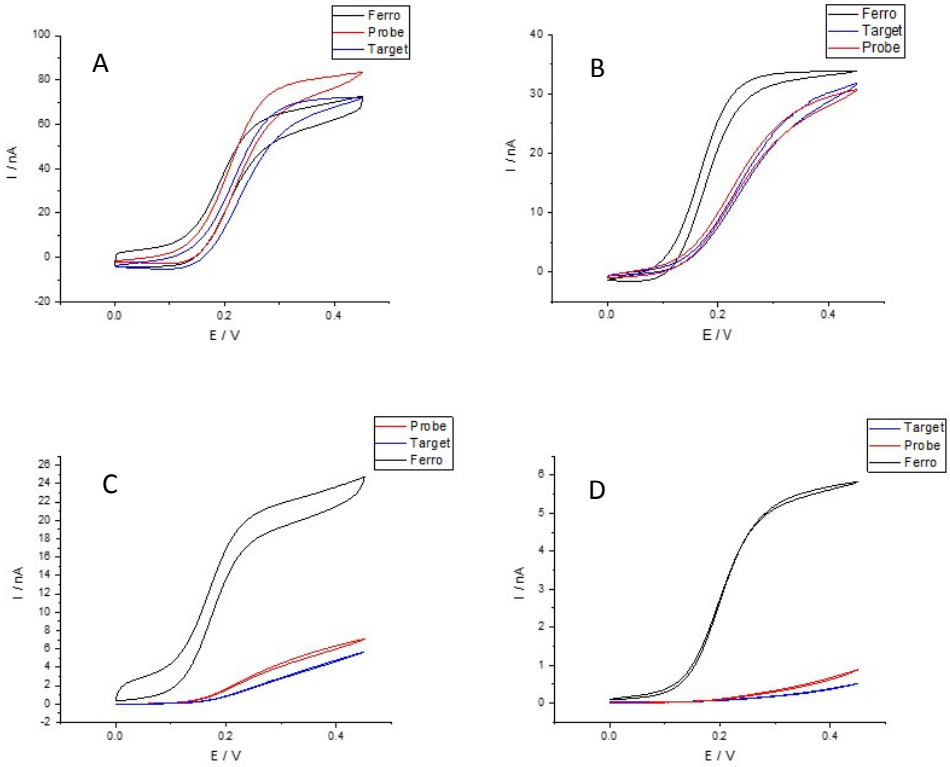

Figure S1. Cyclic voltammetry in 5 mM potassium ferrocyanide + 10 mM KCl following cleaning (black) probe modification (red) and 100 nM DNA target addition. For r = (A) 50, (B) 25 (C) 15 & (D) 5 µm

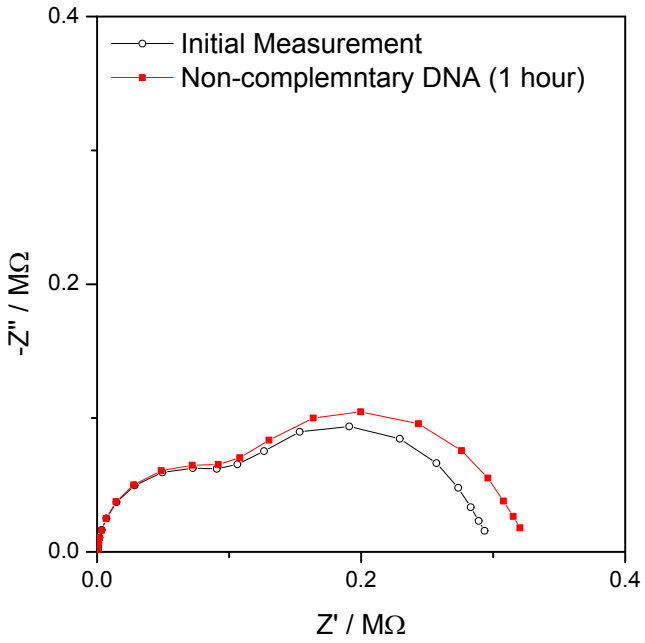

Figure S2. EIS performed in 5 mM potassium ferrocyanide + 10 mM KCl before and after hybridisation with a non-complementary oligonucleotide sequence using a square microelectrode with an edge length of 30 µm.